International Microbiology (2022) 25:745–758
https://doi.org/10.1007/s10123-022-00258-5

ORIGINAL ARTICLE

Bioremediation potential of hexavalent chromium-resistant *Arthrobacter globiformis* 151B: study of the uptake of cesium and other alkali ions

Olia Rcheulishvili[1] · Nunu Metreveli[1] · Revaz Solomonia[2] · Lia Tsverava[2] · Hoi-Ying Holman[3]

Received: 7 December 2021 / Revised: 4 May 2022 / Accepted: 7 June 2022 / Published online: 29 June 2022

Abstract

Cesium (Cs^+) enters environments largely because of global release into the environment from weapons testing and accidents such as Fukushima Daiichi and Chernobyl nuclear waste. Even at low concentrations, Cs^+ is highly toxic to ecological receptors because of its physicochemical similarity to macronutrient potassium (K^+). We investigated the uptake and accumulation of Cs^+ by *Arthrobacter globiformis* strain 151B in reference to three similar alkali metal cations rubidium (Rb^+), sodium (Na^+), and potassium (K^+). The impact of hexavalent chromium (Cr^{+6}) as a co-contaminant was also evaluated. *A. globiformis* 151B accumulated Cs^+ and Cr^{6+} in a time-dependent fashion. In contrast, the uptake and accumulation of Rb^+ did not exhibit any trends. An exposure to Cs^+, Rb^+, and Cr^{+6} triggered a drastic increase in K^+ and Na^+ uptake by the bacterial cells. That was followed by the efflux of K^+ and Na^+, suggesting a Cs^+ "substitution." Two-dimensional gel-electrophoresis of bacterial cell proteomes with the following mass-spectrometry of differentially expressed bands revealed that incubation of bacterial cells with Cs^+ induced changes in the expression of proteins involved in the maintenance of cellular homeostasis and reactive oxygen species removal. The ability of *A. globiformis* 151B to mediate the uptake and accumulation of cesium and hexavalent chromium suggests that it possesses wide-range bioremediation potential.

Keywords Bioremediation · Alkali ions · Metal toxicity and uptake · *Arthrobacter globiformis* 151B · Proteome changes · Cesium

Introduction

Alkali metal element cesium (Cs^+) is characterized by physicochemical similarity to macronutrient potassium (K^+). It has capacity to interact with many ecological receptors, exerts its deleterious outcome, and damages the cells (Sheahan et al. 1992; Avery 1995a, 1995b; Kang et al. 2017; Adams et al. 2019). There are more than 21 isotopes of cesium (Djedidi et al. 2014). The stable isotope cesium-133 ($^{133}Cs^+$) cation occurs naturally in the environment mainly from erosion and weathering of rocks and minerals like the aluminosilicate and pollucite (Djedidi et al. 2014). It is also released into the air, water, and soil through the mining and milling of ores (White and Broadley 2000).

The most hazardous radioactive isotopes: cesium-134 ($^{134}Cs^+$) with half-life 2.06 y, cesium-135 ($^{135}Cs^+$) with half-life 2.3×10^6 y, and cesium-137 ($^{137}Cs^+$) with half-life 30.2 y were released and emitted β and γ radiations during their decay processes throughout nuclear-power plant accidents of Chernobyl and Fukushima Daiichi (Djedidi et al. 2014; Burger and Lichtscheidl 2018; Zok et al. 2021). Radiocesium isotope $^{134}Cs^+$ is an activation product arising directly from the bombardment of stable cesium with neutrons, while $^{135}Cs^+$ and $^{137}Cs^+$ are fission products formed after thermal neutron fission of spent fuel containing Uranium-235 isotope (Burger and Lichtscheidl 2018). Cs^+ is highly mobile. Due to its volatility, it could travel long distances before settling in its aqueous form on earth, leading to widespread

This work is dedicated to my (Olia Rcheulishvili) late supervisor and dear person Dr. Nelly Tsibakhashvili.

✉ Olia Rcheulishvili
olia.rcheulishvili.1@iliauni.edu.ge

[1] Institute of Biophysics, Ilia State University, 3/5 Kakutsa Cholokashvili Ave, Tbilisi 0162, Georgia

[2] Institute of Chemical Biology, Ilia State University, 3/5 Kakutsa Cholokashvili Ave, Tbilisi 0162, Georgia

[3] Lawrence Berkeley National Laboratory, One Cyclotron Road, Berkeley, CA 94720, USA

contamination of miles of urban, agricultural, and forested areas, ponds, and rivers (Koarashi et al. 2016; Linnik et al. 2013; Shaw et al. 2003; Yasunari et al. 2011) After radioactive cesium fallout is deposited into the soil, it forms cesium compounds, mainly salts, which are highly water-soluble. Cesium binds to soil particles strongly and little is leached into the groundwater (Adams et al. 2015). It remains within the top layers of soils and is taken up slowly by plants, received by humans, and other ecological receptors.

The persistence of Cs^+ in the bio-environments is of concern mostly because of its abundant fission product with gamma emissions which lead to the generation of reactive oxygen species (ROS) in cells via radiolysis of water, in addition to inducing mutations (Oh et al. 2018; Yu et al. 2015). The removal of cesium is very challenging: conventional methods such as ion exchange, chemisorption-based soil-sorption techniques, or membrane filtration are limited by their complexities, high costs, and vulnerability to secondary pollution (Takei et al. 2014; Wang and Zhuang 2019; Yang et al. 2014). Bioremediation methods based on the use of microorganisms, microalgae, or plants to sequester and remove Cs^+ have long been considered a primary and sustainable solution (Djedidi et al. 2014; Burger and Lichtscheidl 2018; Kim et al. 2019; Zhang et al. 2014). The passive adsorption of Cs^+ on the cell surface or in the extracellular matrix is expected not to be of significant effects. In contrast, active uptake and intracellular accumulation of Cs^+ can be dangerous because of the similarity of hydration energy, atomic radius, and valence between Cs^+ and the macronutrient K^+. Cs^+ has capacity to compete with K^+ via the metabolic-dependent K^+ transport systems. Bacteria use different transporters powered by electrochemical potential or ATP hydrolysis and protein phosphorylation-dephosphorylation cycle to uptake and maintain their intracellular K^+ concentration for essential cellular functions, including maintenance of cell turgor and homeostasis, adaptation to osmotic conditions, and activation of cytoplasmic enzymes (Bossemeyer et al. 1989; Epstein 2003; Grundling 2013). The presence of intracellular Cs^+, even at relatively low concentration, could disrupt the Na^+/K^+ homeostasis in cells, leading to an uncontrolled formation of ROS via the Fenton reaction that produces hydroxyl radicals and reactive nitrogen species (RNS), causing oxidative damage to biological macromolecules such as DNA, proteins, and lipids (Valko et al. 2016).

The primary challenge of using microorganisms to remediate Cs^+ is Cs^+-induced ROS, which can impair or even eliminate the bioremediation potential of microorganisms. Following the Fukushima Daiichi nuclear power plant (FDNPP) accident that released large amounts of radioactive substances into the environment and contaminated the soil, some studies reported that terrestrial cyanobacteria collected from polluted soil, which include a *Nostoc commune* (Sasaki et al. 2013) and a consortium of cyanobacteria biomats (Yamamoto et al. 2015) absorbed and accumulated the highest quantities of Cs^+. The widely distributed cyanobacteria have developed through a long evolution history both enzymatic (such as superoxide dismutases -SODs) and non-enzymatic (such as the carotenoid antioxidants) defenses to prevent the accumulation of ROS produced during photosynthesis (Latifi et al. 2009; Mironov et al. 2019). It appears that these ROS adaptive outcomes promote the Cs^+ sequestration in cyanobacteria. Several multi-stress resistant microorganismss isolated from environmental samples near sites of the nuclear reactor have also shown to be capable of Cs^+ uptake and accumulation, which include a couple of species of *Rhodococcus* (Ivshina et al. 2002; Takei et al. 2014), and a bacterium *Exiguobacterium acetylicum* (Oh et al. 2018).

Analyses and the investigation of stable cesium ^{133}Cs and its behavior toward living things are a long-term indicator of radiocesium (^{137}Cs, ^{134}Cs) management in ecosystems, its retention, and uptake (Yoshida et al. 2000; Cook et al. 2007; Burger and Lichtscheidl 2018).

Arthrobacteria is ubiquitous in environments. It is evidenced that *Arthrobacter* sp. isolated from Cr or uranium (U) contaminated rocks, soil, and sediments tolerated ROS and accumulated Cr and U intracellularly as precipitates (Holman et al. 1999; Suzuki et al. 2002; Tsibakhashvili et al. 2011). It is not clear whether these bacteria which have adapted to ROS stress and metal toxicity can be used to remediate Cs^+.

In this study, we investigated *Arthrobacter globiformis* 151B, an aerobic, basalt-dwelling, endolithic, Cr^{+6}-resistant bacteria, isolated from the Kazreti region in Georgia polluted with chromium, cadmium, copper, zinc, nickel, and vanadium (Tsibakhashvili et al. 2002, 2011). The detailed information about Kazreti region is provided in the supplementary file "Kazreti".

The potential of *A. globiformis* 151B to uptake Cs^+, versus the other three similar Group I alkali metal cations Rb^+, K^+, and Na^+, was assessed. The impact of Cr^{6+} as a co-contaminant was also evaluated. To analyse how the exposure to Cs^+ could modify the state of proteins in *A. globiformis* 151B, the proteomic analysis of *A. globiformis* 151B was performed to gain additional insights into the molecular mechanism associated with its response to Cs^+. As an analog of radioactive ^{137}Cs, stable isotope ^{133}Cs was used.

Materials and methods

Reagents and chemicals

Tryptic Soy Broth (TSB), Tryptic Soy Agar (TSA), K_2CrO_4, CsCl, RbCl, and chemicals used in sample preparation for 2-D electrophoresis or mass spectrometry (MS) experiments

were purchased from Sigma and Thermo Fisher (ACS reagent grade).

Bacterial culture and growth conditions

A. globiformis 151B was isolated previously from basalts in the Kazreti region of Georgia polluted with a mixture of heavy metals (Tsibakhashvili et al. 2011). Cells of *A. globiformis* 151B were grown aerobically in 250-ml Erlenmeyer flasks as a 100-ml suspension in TSB broth at 21℃ with constant shaking at 100 rpm until the time: $t = 1.5$, 6, 12, 24, 48, 72, 96 h.

Metal uptake experiments

The metal uptake and accumulation experiments were carried out by subjecting cells to five different experimental conditions for 96 h: (1) cells in a liquid culture free of Cr^{6+}, Cs^{+}, and Rb^{+} (Controls); (2) cells with the addition of only Cs^{+}; (3) cells with the addition of only Rb^{+}; (4) cells with the addition of Cs^{+} and Rb^{+}; and (5) cells with the addition of Cs^{+} and Cr^{+6}. Cr^{+6}, Cs^{+}, and Rb^{+} were added simultaneously to the bacterial batch cultures as K_2CrO_4, CsCl, and RbCl respectively. To study the effect of coexisting action of Cr^{+6} and another toxic and potentially radioactive element ions like Cs^{+} and Rb^{+} on the uptake of each other by *A. globiformis* 151B, we added 500 mg/L of Cs^{+} and Rb^{+} and 50 mg/L Cr^{+6} to the bacterial cells. We chose a low concentration of Cr^{6+} (50 mg/L) to avoid the possible decrease of bacterial biomass. It is known that high concentrations of Cr^{6+} can lower the biomass of bacteria (Tsibakhashvili et al. 2011). The experiment was performed in triple replicates and the samples from each condition were harvested at $t = 1.5$, 6, 12, 24, 48, 72, 96 h (Figs. 1–3 and 5–7). The media were not replenished during the experiment. Culture growth was observed by measuring optical density at 490 and 590 nm and by weighing bacterial biomass after washing and drying procedures (lyophilization) (Fig. 3). The wavelengths for the OD measurements were selected according to the approved methodology for *Arthrobacter globiformis* 151B growth measurements (Asatiani et al. 2004; 2018). Bacterial viability and resistance against Cs^{+}, Rb^{+}, and Cr^{+6} were measured by counting colony-forming units on metal-containing agar plates.

Sample preparation

At defined times after the start of cultivation (see above), bacterial cells were harvested from the nutrient medium by centrifugation (3,000 g, 10 min, 4℃), rinsed three times in phosphate-buffered saline (PBS), and prepared for the further analyses. For determination of the metal accumulation capacity by bacteria itself, the wet biomass of bacterial pellet

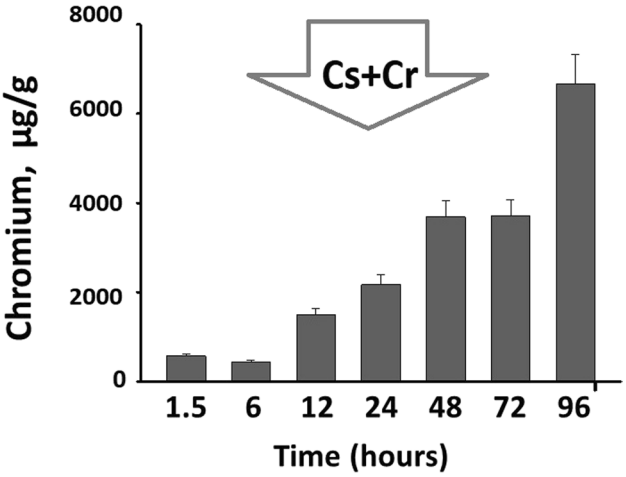

Fig. 1 Time course of chromium uptake by *Arthrobacter globiformis* 151B cells, grown in $Cs^{+}+Cr^{6+}$ containing medium (500 mg/L of Cs^{+} and 50 mg/L Cr^{6+}). Bacterial exposure time with metals in growth media is indicated on x-axis. The mean values ± standard error of the means (SEM) of the total Cr^{6+} concentrations are indicated on the y-axis and represent uptaken Cr^{6+} in µg per gram of bacterial dry mass. The data are provided as mean values ± standard error of the mean (SEM). The details of the statistical analysis are provided in supplementary table S1

after centrifugation and washing procedures were lyophilized according to the method described by Mosulishvili et al. (2002); Tsibakhashvili et al. (2009); and Kalabegishvili et al. (2013). Bacterial biomass (wet) samples were placed in the cylindrical chamber of the lyophilizer; at the same time, bottom part of the chamber is filled with SiO_2 new regenerated granules, which removes the moisture from the cells. Concurrently, liquid nitrogen fixes the biological samples in a short time by freezing them as the metal trunk of the adsorption-condensation lyophilizer chamber is immersed in a liquid nitrogen balloon. The pressure in the chamber is below 0.2 atm. The stationary temperature of the lyophilization process is – 17℃; the fast, strong cooling of the SiO_2 from chamber trunk in liquid nitrogen determines strong evaporation of liquid from samples (Kalabegishvili et al. 2013). Dried cells were weighed, ashed in nitric acid, diluted with bi-distilled water, and analyzed by spectral analytical methods. Sample preparation for proteomic analyses is provided in the "Proteomic study" section.

Spectral analysis

Atomic absorption (AA) and atomic emission (AE) spectrometry were carried out to measure the concentrations of Cr, Cs, Rb, Na, and K at each harvesting time point. The concentrations of Cr and Na were determined by the AA spectrometry method. AE spectrometry method was used to determine Cs, Rb, and K concentrations. The spectrum of the acetylene-air flame was used in the determination of the

metals by AA/AE spectrophotometry by Analyst 800 Perkin Elmer. The detection was carried out at the wavelength of 357.9 nm for chromium, 589.0 nm for sodium, 766.49 nm for potassium, 780.02 nm for rubidium, and 852.1 nm for Cs.

Proteomic study

Comparative 2-D gel-electrophoresis experiments were carried out at 72 h after the start of cultivation. This time point is toward the end of time-dependent studies and should reveal the stable changes of treatment effects. At 72 h after the start of cultivation, control cells and cells grown on Cs containing medium were harvested from the nutrient medium by centrifugation (3,000 g, 10 min, 4℃), rinsed three times in PBS solution, and prepared for 2-D electrophoresis.

Preparation for 2-D electrophoresis

Bacterial pellets were resuspended in buffer (20 mM Tris–acetate, pH 7.8, 20 mM NaCl, 2 mM EDTA, 100 µg/ml lysozyme). Samples were incubated for 30 min at 37℃ with intermittent vortexing. 9 M urea, 4% Tween 40, 2% pharmalyte, 2% mercaptoethanol, and 2% protease inhibitor (bacterial) were added, and lysates were centrifuged at 15,000 × *g* for 30 min at 4℃. The supernatant was collected and protein concentration was quantified by a micro-BCA kit (Pierce, Thermo Scientific) in quadruplicate for both samples with the appropriate buffer controls. The 2-D electrophoresis was carried out as described in the "2-D electrophoresis—principles and methods" (https://www.mcgill.ca/cian/files/cian/ge_2d_manual.pdf) with minor modifications according to Nozadze et al. 2015.

Sample preparation and isoelectric focusing

Isoelectric focusing (IEF) strips (linear pH 3–10 and pH 4–7) were rehydrated in 8 M urea, 0.5% Triton X-100, 0.5% Pharmalyte 3–10, and 30 mM Destreack reagent overnight. Protein samples (40 µg) were loaded onto rehydrated strips in buffer containing 7 M urea, 2 M thiourea, 2% Triton X-100, 0.1% ASB-14, 2-mercaptoethanol, 2% Pharmalyte 3–10, bromophenol blue, and 2% protease inhibitor. IEF was carried out at 500 V for 3 h and 3,500 V approximately for 18 h.

Sample analysis

Equilibration, SDS electrophoresis, staining, scanning, in gel-digestion (differentially expressed spots were cut out and analyzed by MS for the protein identification), and MS analysis experiments were carried out essentially as described by Nozadze et al. (2015). MS experiments were performed using LTQ Fleet ion trap fitted with nanospray ion sources (Thermo Fisher). MS/MS spectra data were analyzed using SEQUEST (Proteome Discoverer 1.4, Thermo Fisher), searching against UniProt UniRef100 *Arthrobacter* species protein databases.

Statistical analysis

The data of the accumulated metal concentrations in different experimental groups were analyzed using one-way and two-way Analysis of Variance ANOVA. The factors were growth condition and time of incubation. Planned comparisons were done by Student's *t*-test. All statistical tests were two-tailed and all significant differences ($P < 0.05$) are reported. Each group from each time point consisted of 3 parallel samples. All of the calculations were done by software "Minitab 16" (https://www.minitab.com/en-us/products/minitab/).

Results and discussion

Uptake of Cr^{+6}

It is known that different metal ions can affect the uptake processes of any other metal by synergetic or antagonistic interactions (Chandrangsu et al. 2017; Tsibakhashvili et al. 2011). *Cyanobacteria* increased the uptake process of radioactive Cs^+ under the influence of K^+ high concentrations (Yamamoto et al. 2015).

The time course of Cr^{6+} uptake by *A. globiformis* 151B cells with the existence of Cs^+ is shown in Fig. 1. The effect of the factor of time on Cr^{+6} uptake was significant: $F(6, 20) = 43.39$, $P < 0.0001$. The uptake of Cr^{+6} in the presence of Cs^+ significantly increased in a time-dependent fashion starting at the 12 h time point and reached the maximum at the end-point of experiments. The data of detailed statistical analysis are provided in Supplementary Materials (Table S1). Cr loading became more effective in the presence of 500 mg/L Cs^+ in the growth medium. Cr concentration in cells was increased with time and reached up to 7000 µg/g. It was reported in our previous studies that *A. globiformis* 151B reduced Cr^{6+} to Cr^{3+} and its reduction began after several hours from starting of their concomitant exposure (Tsibakhashvili et al. 2011). It is reasonable to consider that a high amount of total accumulated Cr^{6+} for 96 h of incubation in the presence of Cs^+ was reduced to the Cr^{3+} form.

Cs^+ uptake and proteomic changes induced by Cs^+ exposure

For microorganisms, Cs^+ is the most toxic among the alkali metal ions (Wackett et al. 2004). Bacterial normal growth does not require the existence of Cs^+or Rb^+ ions in the

growth medium, but they can be used in case of lack of K^+ to restore and maintain normal cellular development (Brown and Cummings 2001; Jasper 1978; Wackett et al. 2004). Cs^+, Rb, or Cr^{6+} treated cells of *A. globiformis* 151B, effectively uptake Cs^+ ions and its concentration is increasing according to the time. Two-way ANOVA analysis of Cs^+ concentration data revealed that the effects of factors – growth condition and incubation time were significant: F (2, 62) = 171.76, $P < 0.0001$ and F (6, 62) = 30.4, $P < 0.0001$ respectively. The interaction between these two factors was also significant F (12,62) = 4.76, $P < 0.0001$. The data of detailed statistical analysis of planned comparisons are provided in Supplementary Materials (Tables S2-S4).

The data of Cs^+ concentration changes in bacterial cells in a time-dependent fashion are shown in Fig. 2. One and half hours (1.5 h) and six hours (6 h) after the start of incubation Cs^+ concentration is significantly increased with the presence of Rb^+ or Cr^{+6} ($P < 0.05$). At the 1.5 h time point, the effect of Cr^{+6} is stronger compared to Rb^+, whereas at 6 h, the difference between these two conditions is not significant. At each of the following time points: 12 h, 24 h, 48 h, 72 h, and 96 h after the start of incubation Cs^+ concentrations are significantly higher in $Cs^+ + Cr^{+6}$ treated cells compared to only Cs^+-treated cells ($P < 0.05$). At three time points: 24 h, 48 h, and 72 h Cs^+ concentration are also significantly increased by Rb^+ compared to only Cs^+-treated cells. Thus, the general tendency is the time-dependent increase in Cs^+ uptake and accumulation. Cs^+ transport is mostly associated with different specific monovalent ion transporters and its toxicity is due to the reduction of K^+

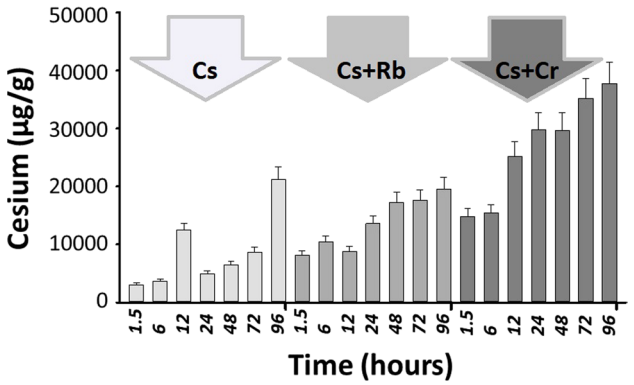

Fig. 2 Time course of Cs^+ uptake by *A. globiformis* 151B cells, grown in different growth mediums: Cs containing medium, Cs + Rb containing medium, Cs + Cr containing medium. Corresponding media contain: 500 mg/L of Cs^+, 500 mg/L of Rb^+ and 50 mg/L of Cr^{6+}; Bacterial exposure time with metals, in growth media is indicated on x-axis. The mean values ± standard error of the means (SEM) of Cs^+ concentrations are indicated on the y-axis and represent uptaken Cs^+ in µg per gram of bacterial dry mass. Two-way ANOVA analysis of Cs^+ concentration data: factor-condition F (2, 62) = 171.76, $P < 0.0001$ and effect of factor-time: F (6, 62) = 30.4, $P < 0.0001$

uptake capability by bacteria, or increase the efflux of K^+ (Bossemeyer 1989; Jung et al. 2001; Wackett et al. 2004). In these experiments, during the uptake process of Cs^+ by *A. globiformis* 151B, the efflux of K^+ or Na^+ is observed (see below; Figs. 6, 7). Zhang et al. (2014) have indicated that the Cs^+ uptake process by bacteria was mediated by the K^+ transport system and was characterized by a saturation phenomenon and the uptake process was inhibited dose-dependently by K^+. In our study, the intracellular concentrations of K^+ and Na^+ have decreased after time, when cells were treated with Cs, Rb, or Cr^{6+}. But the same heavy metals do not affect the Cs^+ uptake process for cells, and Cs^+ intracellular concentration has increased with time. It is known that at low concentration, Cs^+ can stimulate bacterial growth in the absence of K^+ (Jasper 1978; Wackett et al. 2004), but it can affect plant functioning and reduce its growth via activating the defense mechanism against oxidative stress (Atapaththu et al. 2016). According to our experiments, we can suggest that the induced oxidative stress by Cs^+ or Cr^{6+} with their single or concomitant ($Cs^+ + Cr^{6+}$, $Cs^+ + Rb^+$) action also affects the biomass of *A. globiformis* 151B at 96 h of its development for all types of growing conditions. Almost at every time point, Rb^+ and ($Rb^+ + Cs^+$) even increase the biomass of cells compared to the control. The only exception is Cr^{6+}, which reduces the biomass of *A. globiformis* 151B at every time point (Fig. 3).

Cs^+ is known to have a large hydrated ion radius. The free mobile single electron can react with water and oxygen to form reactive oxygen species, leading to the activation of the antioxidative defense system in plants or bacteria (Atapaththu et al. 2016). Cs^+ can easily replace K^+ ion and, on the other hand, it activates certain enzymes, which are necessary for bacterial survival during increased ROSs (Andersson and Mowbray 2002; Wackett et al. 2004). *A. globiformis* 151B effectively survives under the strongest oxidative stress which is caused by Cr^{6+} and Zn^{2+} concomitant prolonged exposure with the help of the antioxidant enzyme (SOD and catalase) activity during 96 h (Asatiani et al. 2018).

Comparative 2–D gel electrophoresis approach revealed the only 8 significantly upregulated proteins in *A. globiformis* 151B cells, grown on Cs^+ containing medium compared to control cells (Fig. 4). Comparative 2-D gel-electrophoresis experiments were carried out at 72 h after the start of treatment. The software used for the comparison of the images (see the "Proteomic study" section) calculates the relative volumes of the protein spots. Some proteins spots were eventually decreased, but they were not identified as significantly decreased proteins and "escaped" further MS analysis and identification. The protein identities of differentially expressed spots revealed by MS analysis are provided in Table 1. A total of 500 mg/L Cs^+ concentration increased the expression of proteins with different functions. We hypothesize that exposure of Cs^+ causes oxidative stress,

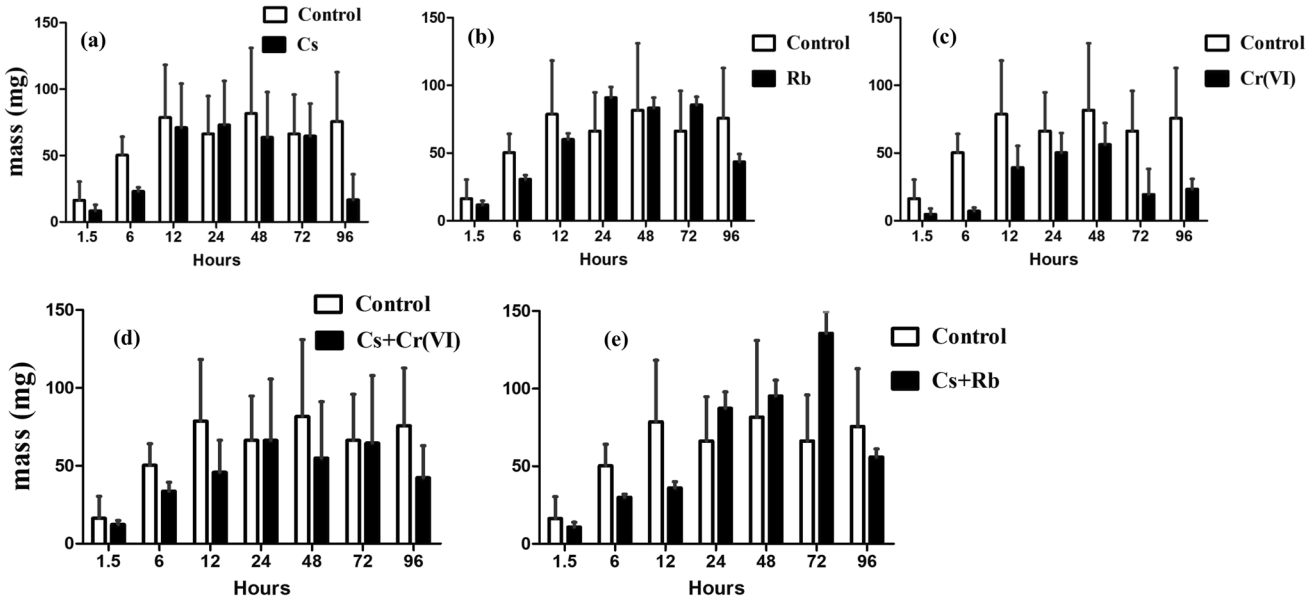

Fig. 3 The influence of metal ions and their exposure time on bacterial biomass: (**a**) influence of Cs^+ ions, (**b**) influence of Rb^+ ions, (**c**) influence of Cr^{6+} ions, (**d**) influence of Cs^+ and Cr^{6+} joint action, (**e**) influence of Cs^+ and Rb^+ joint action on bacterial growth masses. Bacterial exposure time with metals in growth media is indicated on x axis, while y axis denotes the biomass of bacterial cells

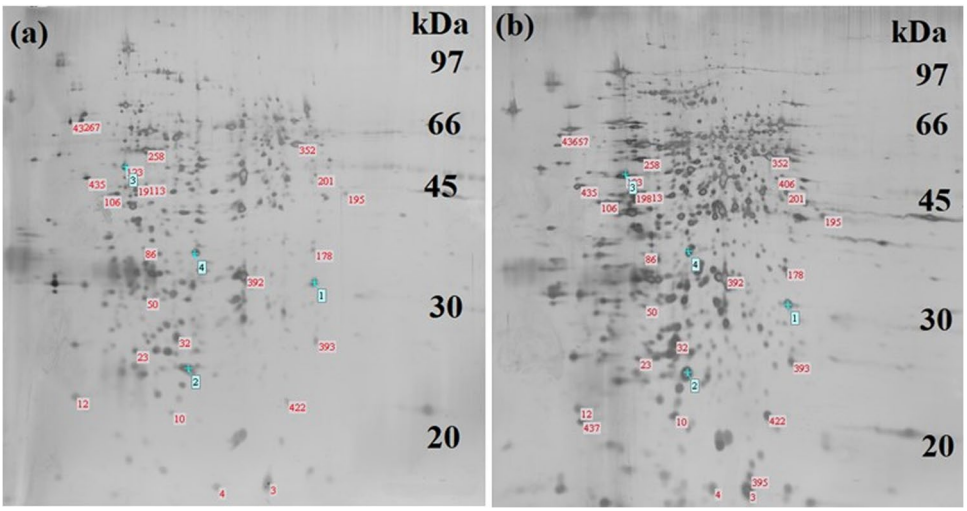

Fig. 4 Representative images of silver-stained 2-D gel electrophoresis gels on strips with pH linear gradient 4.0–7.0 of *A. globiformis* 151B, protein extracts 72 h of growth. (**a**) Protein extracts from control cells grown without Cs containing medium. (**b**) Protein extracts of cells grown on Cs containing medium (500 mg/L). Light green color points represent the marks done by the ImageMaster 2-D platinum 7.0 software. They indicate the matched starting identical points (ID similarities) for matching the rest of the protein ID-s (indicated in red), to find the significantly differentially expressed protein bands (dots) between (a) or (b) gel figures

formation of ROS, or other free radicals. It can also cause lipid peroxidation and further membrane damage. On the other hand, Cs^+ activates the bacterial antioxidant defense system. MS analyses revealed that Cs^+ exposure induces the upregulation of several proteins which are mainly involved in oxidative stress response reactions and maintenance of the cellular ion homeostasis. Functions of the upregulated proteins are associated with oxidoreductase activity, peroxiredoxin activity (peroxiredoxin has antioxidative property and reduces oxidation of lipids), metal-ion binding, ATP synthesis, and hydrolysis activity. The upregulation of these proteins could normalize transmembrane active transport of different ions or compounds, lipopolysaccharide, and peptidoglycan biosynthetic processes and in general to restore the "damaged shape" of bacterial cell wall/membrane and protect bacterial DNA from oxidative damage.

Table 1 The list of significantly differentially expressed proteins in Cs^+-treated bacteria compared to the control groups. The data for the spots coinciding by location (pI and molecular weight) from different experiments were analyzed by a two-tailed *t*-test for significant differences between the two groups; the significance level was set at 5%. All significant changes are more than 1.5-fold. ↑ indicates the upregulation of expression. For each protein, the Uniprot identifier is also indicated

Proteins upregulated in Cs treated cells versus the control cells	Direction of changes	Molecular/biological functions of Proteins upregulated in Cs treated cells versus the control cells	Proteins upregulated in Cs treated cells versus the control cells	Direction of changes	Molecular/biological functions of Proteins upregulated in Cs treated cells versus the control cells
DNA protection during starvation protein (Dps) UniProtKB - A0A0K2QYH4 (A0A0K2QYH4_9MICC)	↑	oxidoreductase activity, oxidizing metal ions, Ferric ion binding	Histidine kinase UniProtKB - A0A1F1UEA2 (A0A1F1UEA2_9MICC)	↑	ATP binding, metal ion binding, polyphosphate kinase activity, polyphosphate biosynthetic process
TetR family transcriptional regulator UniProtKB - A0A221NFI1 (A0A221NFI1_9MICC)	↑	DNA binding, negative regulation of transcription, DNA template, response to antibiotic	Uncharacterized protein UniProtKB - A0A0S2M2X3 (A0A0S2M2X3_9MICC)	↑	ATP-ase activity, transmembrane transport, Lipase activity, lipid metabolic process, outer membrane component
Carboxymuconolactone decarboxylase UniProtKB - A0A0Q9MZX1 (A0A0Q9MZX1_9MICC)	↑	4-carboxymuconolactone decarboxylase activity, aromatic compound catabolic process, peroxiredoxin activity	ATP-binding protein involved in chromosome partitioning UniProtKB - A0A1G8C159 (A0A1G8C159_9MICC)	↑	ATP binding, DNA binding, chromosome condensation activity, DNA replication activity
RNA polymerase subunit sigma-70 UniProtKB - A0A0Q9N0X6 (A0A0Q9N0X6_9MICC)	↑	Response to osmotic stress, DNA binding, DNA-binding transcription factor activity, DNA-directed 5'-3' RNA polymerase activity, magnesium ion binding, zinc ion binding, transcription, DNA-templated, sigma factor activity, transcription initiation from bacterial-type RNA polymerase promoter	UncharacterizedN-acetyltransferase UniProtKB - A0A1P8M7R8 (A0A1P8M7R8_9MICC)	↑	Glucosamine-1-phosphate N-acetyltransferase activity, magnesium ion binding, UDP-N-acetylglucosamine diphosphorylase activity, cell morphogenesis, cell wall organization, lipid A biosynthetic process, lipopolysaccharide biosynthetic process, peptidoglycan biosynthetic process, regulation of cell shape, UDP-N-acetylglucosamine biosynthetic process

Rb^+ uptake

The effect of the factor "growth condition" on Rb^+ uptake is significant [F (1, 41) = 11.02, P = 0.003]. The effect of time is also significant F (6, 41) = 9.29, $P < 0.0001$), whereas the interaction between these factors is not significant. The general tendency for Rb^+ concentration is the time-dependent decrease (Fig. 5). The data of detailed statistical analysis are provided in Supplementary Materials (Tables S5, S6). At 6 h after the start of incubation, the Rb^+ concentration is significantly higher with the presence of Cs^+ in the medium compared to the cells incubated only with Rb^+ ($P < 0.05$). At the final time points of experiments (96 h) for both conditions, the Rb^+ concentrations are significantly less compared to initial corresponding values ($P < 0.05$). For the Rb + Cs, the same tendency is also significant at 72 h after the start of incubation.

K^+ and $Na.^+$ uptake

The time-course of K^+ uptake by bacterial cells under the influence of toxic metals and their combination in a time-dependent fashion are shown in Fig. 6. Two-way ANOVA analysis of K^+ concentration data revealed that the effects of factor- "growth condition" [F (4,104) = 15.46, P = 0.0001] and factor- "time" [F (6, 104) = 77.23, $P < 0.0001$] and the interaction between these factors are significant [F

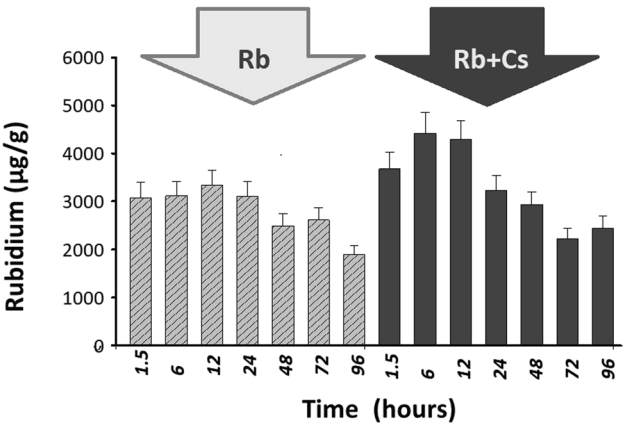

Fig. 5 Time course of Rb^+ uptake by *Arthrobacter globiformis* 151B cells, grown in different growth mediums: Rb^+ containing medium, Rb + Cs containing medium (corresponding media contain: 500 mg/L of Cs^+ and 500 mg/L of Rb^+). Bacterial exposure time with metals in growth media is indicated on x-axis. The mean values ± SEM of Rb^+ concentrations are indicated on the y-axis and represent uptaken Rb^+ in µg per gram of bacterial dry mass

(24,104) = 2.80, $P = 0.0001$]. The data of detailed statistical analysis are provided in Supplementary Materials (Tables S7–S11).

One and half hours (1.5 h) after the start of incubation, all tested metals and their combinations (Cs^+, Rb^+, $Rb^+ + Cs^+$ and, $Cs^+ + Cr^{6+}$) significantly (for all comparisons $P < 0.05$) increase K^+ levels compared to control cells. The increase is in the range of 30–40%.

Higher levels of K^+ for 1.5 h are observed in Rb^+ and ($Cs^+ + Rb^+$) groups. Six hours (6 h) after the start of incubation, the differences are exactly the same: the level of K^+ is significantly higher in metal-treated cells compared to the control samples ($P < 0.05$ for each comparison). Twelve hours after the start of incubation, the highest level of K^+ is observed in Cs^+-treated bacterial cells. Twenty-four hours, 48 h, and 72 h after the start of incubation, there are no significant differences between the groups on a 2-tailed test. After 96 h of incubation, the lowest level of K^+ is observed in the ($Cs^+ + Cr^{6+}$) group, which is significantly lower compared to all the other groups. The level of K^+ is also significantly lower in the ($Cs^+ + Rb^+$) group compared to the Rb^+ group.

Two-way ANOVA of Na^+ uptake data revealed that the effects of factor- " growth condition" factor "time" and the interaction of these factors are significant [F (4, 104) = 36.26, $P = 0.0001$; F (6, 104) = 219.1; $P < 0.0001$, F (24, 104) = 18.40; $P = 0.0001$ respectively]. The data of Na^+ uptake in a time-dependent fashion by *A. globiformis* 151B are presented in Fig. 7. The data of detailed statistical analysis are provided in Supplementary Materials (Tables S12–S16F). One and half hours (1.5 h) after the start of incubation, Na^+ concentration is drastically high by the presence of individual metals or their combination in incubation medium compared to the control condition ($P < 0.01$ for all comparisons). Na^+ concentration in cells exposed to single metals (Cs^+ and Rb^+) do not differ. In the case of two metal combinations ($Cs^+ + Rb^+$ and $Cs^+ + Cr^{6+}$), Na^+ concentration is also significantly higher compared to single metal exposed cells ($P < 0.005$ for each comparison). At 6 h after the start of incubation, the concentration of Na^+ is significantly less in control cells compared to all types of treated cells ($P < 0.005$ for all comparisons). At 12 h after the start of incubation, the level of Na^+ is highest in ($Cs^+ + Rb^+$) treated cells which significantly exceeds the corresponding levels in Rb^+ and ($Cs^+ + Cr^{6+}$) treated cells ($P < 0.05$). At 24 h after the start of incubation, in Rb^+- and ($Cs^+ + Rb^+$)-treated cells, the concentration of Na^+ is the highest and exceeds significantly the corresponding values

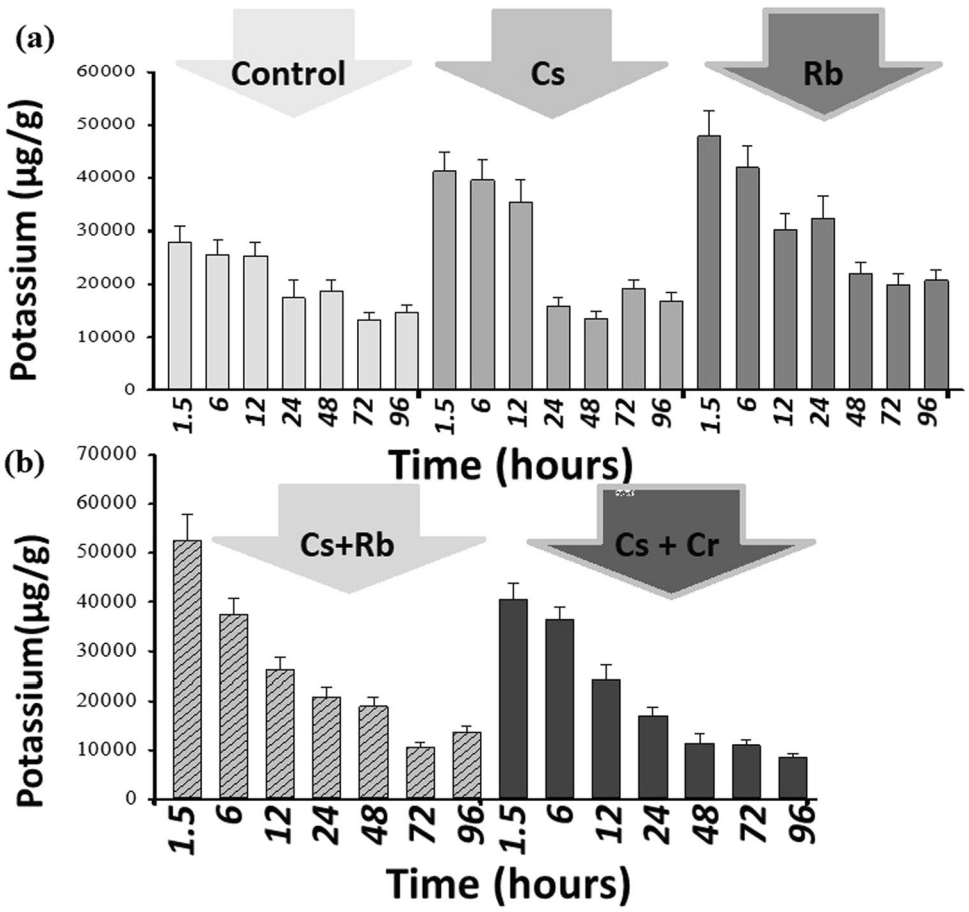

Fig. 6 Time course of K^+ uptake by *A. globiformis* 151B cells, grown in different growth mediums; (**a**) control medium without the addition of metal salts, Cs containing medium, Rb containing medium; (**b**) Cs + Rb containing medium, Cs + Cr containing medium (corresponding media contain: 500 mg/L of Cs^+, 500 mg/L of Rb^+ and 50 mg/L of Cr^{6+}) TS broth contains 1000 mg/L of K^+. Bacterial exposure time with metals, in growth media, is indicated on the x-axis. The mean values ± SEM of K^+ concentrations are indicated on the y-axis and represent uptaken K^+ in µg per gram of bacterial dry mass

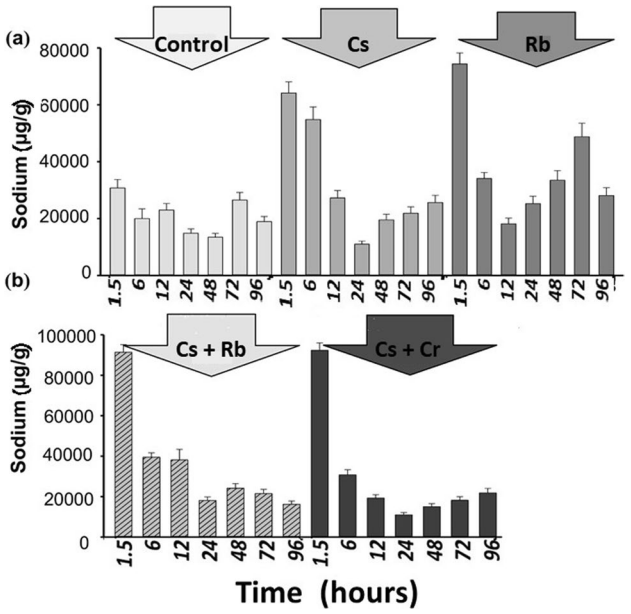

Fig. 7 Time course of Na^+ uptake by *A. globiformis* 151B cells, grown in different growth mediums; (**a**) control medium without the addition of metal salts, Cs containing medium, Rb containing medium; (**b**) Cs + Rb containing medium, Cs + Cr containing medium: (corresponding media contain: 500 mg/L of Cs^+, 500 mg/L of $Rb^+$and 50 mg/L of Cr^{6+}) TS broth contains 1900 mg/L of Na^+. Bacterial exposure time with metals, in growth media, is indicated on the x-axis. The mean values ± SEM of Na^+ concentrations are indicated on the y-axis and represent uptaken Na^+ in µg per gram of bacterial dry mass

in the control, Cs^+, and ($Cs^+ + Cr^{6+}$) cells ($P < 0.05$). At 48 h after the start of incubation, the differences are nearly the same; the highest level of Na^+ is detected in Rb^+-treated cells which significantly exceeds the corresponding values in control, Cs^+, and ($Cs^+ + Cr^{6+}$) treated cells ($P < 0.05$). At 72 h after the start of incubation, the highest level of Na^+ is detected in Rb^+-treated cells which significantly exceed the Na^+ levels in all other studied cells ($P < 0.05$). At 96 h after the start of incubation, no significant differences are observed between the groups.

K^+ ion homeostasis is essential for bacterial survival, osmoregulation, pH homeostasis, protein synthesis regulation, membrane potential adjustment, and electrical signaling (Stautz et al. 2021). There are two interaction phases between metal-treated *A. globiformis* 151B and Na^+ or K^+ ions: (a) Na^+ and K^+ rapid influx and (b) their slow efflux phases. As the concentration of Cs^+ and Cr^{6+} is increased inside bacteria, K^+ and Na^+ gradual efflux start. This may be explained by the activation of different transport systems reported according to different authors (Epstein 2003; Jung et al. 2001; Stautz et al. 2021; Zhang et al. 2014; Stratford et al. 2019). Transport systems can be the passive channels that allow K^+ and Na^+ ions to flow down their electrochemical gradient or the active transporters that use ATP or the proton motive force (pmf) to accumulate ions against their concentration gradient (Stautz et al. 2021). The electrical gradient, together with the chemical proton gradient, on the other hand, provides the pmf, which is necessary for ATP synthesis and various secondary active transport processes (Stautz et al. 2021). Na^+, K^+ influx systems are activated toward the increased extracellular osmolarity and cell turgor after exposure to toxic metals like Cr^{6+}, Cs^+, Rb^+. And the second, Na^+, K^+ efflux systems inside bacteria are activated by reduction intermediate by-products, antioxidant enzyme metabolites, glutathione metabolites, or electrophiles, which are released immediately as bacteria start Cr^{6+} reduction to its Cr^{3+} form and remediation of Cs^+. It is possible that Na^+ and K^+ initial high concentration and following gradual efflux process are the stress responses of the cells to the exposure to toxic metals. This phenomenon is very similar to the prokaryotic paradigm of electrical signal transduction in cellular communities (Prindle et al. 2015; Ram and Lo 2018; Stratford et al. 2019). Ram and Lo (2018) suggest that bacterial cells, their colonies, and biofilms can show similarities to the neuronal cells and networks, as forming graded or action potentials or ion-dependent signaling. Bacterial ionic membrane voltage regulation is seen in gram-positive *B. subtilis* (Aguilar et al. 2007), According to Prindle et al. (2015), bacteria produce biofilms when they experience stress, forming colonies inside the biofilms, produce electrical oscillations; thus, biofilms gain voltage as a whole. Intracellular and extracellular K^+ and Na^+ ions create a gradient in the nutrient medium, in which the bacteria exist. It is known that the K^+ ion has the main role in resting membrane potential formation. It is also known that the resting membrane potential of *E. coli* vesicles is − 75 mV (Schuldiner and Kaback 1975), which is very similar to the voltage of the nervous cell (− 70 mV). According to Stautz et al. (2021), the membrane potential for a metabolizing bacterium is on the order of –150 mV. Inside negative membrane potential is created by the unequal distribution of ions inside or outside the cell. This kind of distribution by one hand is provided by different active transport proteins and consumes 1/2 of the total cellular energy (Milo and Phillips 2015), and by the other hand, the high amount of impermeable negatively charged macromolecules like proteins, RNA, or DNA is present in the cytoplasm and participate in the Donnan potential or membrane resting potential formation (Eisenberg and Crothers 1979). These fixed charges contribute to the membrane potential regardless of the metabolic activity of the bacterium (Stautz et al. 2021). The electrical gradient ψ provided by the electron transport chain of respiring bacteria determines all membrane-permeable-ion distribution across the plasma membrane according to this potential. Cations and anions will flow through the membrane until their free chemical driving force (diffusion free energy according to the concentration gradient) will not equalize to the electrical

potential force according to the Nernst Equation. For K^+, the equilibrium distribution is established by the membrane potential:

$$\Delta\psi = -\frac{RT}{zF}\ ln\ \frac{[K]in}{[K]out} \quad (1)$$

where R is the gas constant, T is the temperature, F is the Faraday constant, and z is the charge of the ion (Glasser 1999; Stautz et al. 2021). Ion diffusion through plasma membrane requires special high permittivity channels for their permeation (Alberts et al. 2002; Cuello et al. 2010). Most of the ionic channels are "gated" ones and are potential dependent: ion flow rate down the concentration gradient is very fast if there is a steep difference between membrane potential and specific ion equilibrium potential (Alberts et al. 2002). There is no net diffusion of ions through the plasma membrane, when there is a little difference between the membrane potential and ions equilibrium potential (Glasser 1999). Bacterial electrical signaling processes are recently studied and have shown that bacterial membrane potential mediates the intra and intercellular signaling, regulating such important physiological processes as biofilm dynamics, mechanosensation, or spore formation (Stratford et al. 2019). Only a few recent discoveries indicate of bacterial membrane-potential excitation dynamics and a few is known about external electrical signals in the context of bacterial electrophysiology (Stratford et al. 2019). For any type of metabolically active cells, including bacteria, during the resting condition, there is a high K^+ intracellular and Na^+ extracellular concentration. An external electrical stimulus can alter the cellular membrane potential according to the Schwan equation:

$$\Delta\psi\ max = 1.5aE\left(1 + (2\pi f\ \tau)^2\right)^{-1/2} \quad (2)$$

where $\Delta\Psi$ max is the induced membrane potential, a is the cell radius, E is the applied field strength, f is the alternating electric field frequency, and τ is the relaxation time of the membrane (Marszalek et al. 1990; Stratford et al. 2019). Stratford et al. provide that, if the electrical stimulus is applied to proliferative bacterial cells, it should lead to the opening of voltage-gated K^+ channels and consequent hyperpolarization due to K^+ efflux. Replacing the typical values of bacterial resting potential $-140 \sim -75$ mV (Feile et al. 1980; Ramos et al. 1977) and threshold potential for Kv ~ -50 mV (Zheng and Trudeau 2015) to the equation can be expected that the depolarization by an electrical stimulus with the field strength of $+35 \sim 120$ mV/μm should open voltage-gated K^+ channels on bacteria (Stratford et al. 2019). It is considered, that toxic metals, like Cr^{6+}, Cs^+, Rb^+ here play the role of excitation stimuli for *A. globiformis* 151B, and bacteria respond with rapid increased K^+ and Na^+influx process. It is known that Na^+ intracellular concentration is increased during the membrane depolarization phase of graded or action potential when cellular excitation stimulus is provided. Prindle et al. (2015) show the change of membrane potential of *B. subtilis*, which was associated with K^+ efflux when K^+ intracellular concentration was 40 times greater than in extracellular side and suggested that K^+ has a role in the synchronized oscillations in membrane potential. Bacteria release K^+ or Na^+ ions to communicate rapidly to neighboring cells about their metabolic state. Their initial high content can be compared to the depolarization phase of action potential and their following gradual efflux to the membrane repolarization and hyperpolarization phases. The simultaneous exposure to the combination of two toxic metals ($Rb^+ + Cs^+$ and $Cs^+ + Cr^{6+}$) has a different effect at later time points; Na^+ and K^+ levels are decreased below the controls. Stautz et al. (2021) describe several scenarios showing the relationship between bacterial metabolism, K^+ chemical gradient, and membrane potential when intracellular K^+ concentration is 300 mM and extracellular concentrations are 0.1 mM, 1 mM, or 100 mM: (a) in K^+ deficient medium, K^+ accumulation can occur against the electrochemical gradient by primary active transport via ATP hydrolysis or by the secondary active transport via H^+ symport proteins. Or (b) via channels, facilitating the thermodynamically favorable movement of K^+ down its electrochemical gradient. In metabolically active bacteria, when Gibbs free energy of electron transport chain (g_{etc}) is greater than Gibbs free energy for K^+ diffusion ($g_k{}^+$), K^+ can be accumulated in the cytoplasm even at low external concentrations. But, when the relative permeability of K^+ ($g_k{}^+$) exceeds that of protons due to a decrease in metabolic activity or K^+ channel opening, the degree of membrane depolarization is determined by the external K^+concentration (Stautz et al. 2021).

Jung et al. (2001) showed that exposure of *E.Coli* with CsCl leads to the decrease of intracellular K^+, which induces upregulation of the kdpFABC operon coding for high-affinity K^+ uptake system. The components of the sensory kinase/response regulatory system proteins kdpD and kdpE are implicated for the operon expression upregulation. We speculate that despite the normal viability of the *A. globiformis* 151B cells, two-metal combination exposure has a profound effect on cell physiology over time and leads to the abovementioned changes in cell homeostasis. In general, bacterial samples tend to accumulate and increase the level of Cs^+ inside bacterial cells during the whole time of cultivation. The Cs^+ uptake is significantly augmented by the additional presence in the medium of Cr^{6+}, whereas Rb^+ presence does not have any significant influence on it (Fig. 2). Cr^{6+} uptake is also gradually increased over time in the presence of Cs^+. Thus, Cr^{6+} and Cs^+ have synergistic effects on their uptake processes. In difference to Cs^+ and Cr^{6+} uptake, Rb^+ intracellular initial level is high and nearly constant when bacterial cells are exposed only to Rb^+ or

together with Cs^+. The different time dependence of studied toxic metals uptake and their different effects on each other convincingly demonstrate that diverse biochemical systems and various metal-resistant mechanisms are involved in their uptake/release.

K^+, Na^+, Cs^+, and Rb^+ differ according to their atomic radius. Alkali metal salts easily dissociate in water and biological fluids and are highly soluble. Their hydration energy, which is associated with the hydration radius, reduces with increasing ions atomic mass (Glasser 1999), so for Na^+, hydration radius (hydration energy) will be larger than for K^+. That is why dehydration of sodium requires more energy than potassium ions, during transportation through the selectivity filter of the potassium ionic channel of the biological cell membrane. Ions of K^+, Rb^+, or Cs^+ do not have the second hydration shell because of their relatively large crystal radius (Mähler and Persson 2012; Smirnov and Trostin 2007). According to Glasser (1999) with a larger distance from the charged nucleus of the ion, the electric field strength will become lower, that is why water dipoles' attractivity strength for large ions will be relatively weak. All of these ions will require separate transport systems, different ionic channels for their selection and transportation, according to their thermodynamically favorable dehydration systems. It is known that there are different transport mechanisms and uptake systems for separate ions, through the plasma membrane of bacterial cell wall (Gadd and Griffiths 1978). Many bacteria possess different uptake systems for K^+ in the biological cell membranes.

Different transport systems for K^+ ions are seen in different bacteria: YugO in *Bacillus subtilis* which can serve electrical signaling in biofilms (Prindle et al. 2015), HpKch from *Helicobacter pylori* (Stingl et al. 2007), and CglK from *Corynebacterium glutamicum* (follmann et al. 2009) can mediate K^+ uptake, and Kch from *Escherichia coli* is suggested to involve in membrane potential adjustment (Ungar et al. 2001). Three types: Kdp, Trk, and Kup K transport systems are detected in *E. coli* (Zhang et al. 2014). Kdp system is reported as a P-type ATPase with a high affinity toward K, with the requirement of ATP and a divalent cation. Mostly, it determines K^+ uptake (Epstein 2003). Second- the Trk system is responsible for K^+ and Rb^+ transport and the third Kup system has a high affinity toward Cs^+ ion (Epstein 2003; Bossemeyer et al. 1989). KcsA is a voltage-dependent ionic channel highly selective for potassium, after activation, up to 10^8 ions per second flow through the channel for approximately 200 ms, until a slow inactivation takes place (Stautz et al. 2021). It seems that *A. globiformis* 151B can possess similar transport systems for K^+ ion. Why Na^+ or K^+ initial concentration in both control and Cs^+, Rb^+, $Rb^+ + Cs^+$, or $Cs^+ + Cr^{6+}$ groups is so high, or why K^+ or Na^+ efflux starts immediately after the beginning of incubation? Potassium and sodium ions appear to be signaling ions, which help the cell for adaptation to elevated osmolarity by activation of some cytoplasmic enzymes (Epstein 2003). Transport systems for K^+ uptake are regulated by ion concentration, increased medium osmolarity, and increased cell turgor (Epstein 2003). Tsibakhashvili et al. (2011) showed that the cell homeostasis under the stress condition is reached by joint action of the resistance mechanism together with normal cellular metabolism, providing the cell to concentrate adequate metal to keep the metal-dependent activities (Bruins et al. 2000; Choudhury and Srivastava 2001; Tsibakhashvili et al. 2011). Increased medium osmolarity and/or high turgor pressure of medium causes activation of the potassium uptake process (Epstein 2003). Intracellular K^+ concentration is determined mostly by the osmolarity of external medium for *E. coli*, *Salmonella*, or other genera of bacteria (Rhoads et al. 1976).

Microorganisms have specific, selective transport systems for alkali ions, which are fast and driven by the chemiosmotic gradient or toxic electrophiles (in case of K^+ efflux systems) (Bossemeyer et al. 1989; Epstein 2003). Very often, Na^+ transportation through biological cell membranes is associated with Na^+/H^+ antiporters, which regulate cytoplasmic pH under stress conditions (Booth et al. 2003; Wackett 2004). According to Ferguson et al. (1997), electrophiles can activate KefB and KefC transport systems in *E. coli*, which leads to K^+ efflux from the bacterial cell. The abovementioned efflux systems protect *E. coli* against the toxic effects of the electrophiles. In *A. globiformis* 151B during the neutralization of some toxic agents like Cs^+, Cr^{6+}, or Rb^+, different reduction by-products are generated, including glutathione metabolites, toxic agents, or other forms of electrophiles. Reduction by-products can activate similar transport efflux systems for K^+ or Na^+. Na^+ and K^+ efflux process can be considered part of the defensive mechanism of *A. globiformis* 151B, as ROS and metal resistant bacteria. Different transport systems are activated during different physiological states for *A. globiformis* 151B. The oxidized products of free radical attack have decreased biological activity of cell, leading to loss of energy metabolism, cell signaling or other major functions (Mahjoub and Roudsari 2012; Juan et al. 2021).

We have demonstrated the uptake process of K^+, Na^+, Cs^+, Rb^+, and Cr^{6+} with concomitant action of Cr^{6+}, Cs^+, and Rb^+ by the cells of *A. globiformis* 151B. According to the obtained data, *A. globiformis* 151B effectively accumulated Cs^+ and Cr^{+6} ions from the environment. Experiments with the exposure to toxic Cs^+, Rb^+, and Cr^{+6} revealed that bacteria had two interaction phases toward K^+ and Na^+: rapid influx and slow efflux phase. The concentrations of K^+ and Na^+ ions in bacteria had the maximum levels in the first hour of their development. As the intracellular concentrations of Cs^+ and Cr^{6+} ions increased (according to the time), the slow removal phase of K^+ and Na^+ takes place.

The gradual efflux of K^+ and Na^+ ions could be considered one of the defensive mechanisms against the oxidative stress induced by Cs^+ or Cr^{6+}. Before bacterial cells accumulated Cs^+ and Cr^{6+} ions, they are metabolically more active and K^+ ions move inside bacteria either by thermodynamically favorable facilitated passive transport or by primary or secondary active transport. After Cs^+ and Cr^{6+} levels inside bacteria increase, oxidative stress takes place, cellular metabolic activity decreased (g_{etc} is less), and K^+ ions begin to move outside the cell down their electrochemical gradient: to adjust the membrane potential, or to cause the membrane depolarization.

Conclusions

In conclusion:

- *A. globiformis* 151B possesses an effective ability to accumulate Cs^+ ions, even in the presence of other toxic metals such as Cr^{6+}.
- *A. globiformis* 151B displays time-dependent adaptive biochemical changes to cope with various combinations of dangerous metals and survives harsh conditions of growth medium: oxidative stress, caused by Cr^{6+} reduction and Cs^+ remediation, causes the decrease of metabolic activity of the cell, which is revealed by the K^+ and Na^+ slow efflux process.
- *A. globiformis* 151B responds to Cs^+ treatment by remarkable changes in proteome compositions. Proteins implicated in osmolar homeostasis maintenance, redox activity, ATP, and DNA binding proteins are significantly upregulated.
- All the above listed indicate that *A. globiformis* 151B has a high potential for both Cs^+ and Cr^{6+} contaminated soil bioremediation and we suggest that these species of bacteria could be successfully used for this process.

Supplementary Information The online version contains supplementary material available at https://doi.org/10.1007/s10123-022-00258-5.

Acknowledgements We acknowledge Dr. Aleksandre Rcheulishvili for helping to perform the spectral analyses.

Author contributions Material preparation, data collection, and analysis were performed by Olia Rcheulishvili. The first draft of the manuscript was written by Olia Rcheulishvili and all authors commented on previous versions of the manuscript. All authors contributed to the study conception and design. All authors read and approved the final manuscript.

Funding Author Olia Rcheulishvili has received research support from Volkswagen Foundation, within the framework of the joint project "Structured Education- Quality Assurance- Freedom to Think"—#04/46 between Georg-August-University of Gottingen and Ilia State University. Other authors declare that no funds, grants, or other support were received during the preparation of this manuscript.

References

Adams E, Chaban V, Khandelia H, Shin R (2015) Selective chemical binding enhances cesium tolerance in plants through inhibition of cesium uptake. Sci Rep 5:1–10. https://doi.org/10.1038/srep08842

Adams E, Miyazaki T, Saito S et al (2019) Cesium inhibits plant growth primarily through reduction of potassium influx and accumulation in arabidopsis. Plant Cell Physiol 60:63–76. https://doi.org/10.1093/pcp/pcy188

Aguilar C, Vlamakis H, Losick R, Kolter R (2007) Thinking about Bacillus subtilis as a multicellular organism. Curr Opin Microbiol 10:638–643. https://doi.org/10.1016/j.mib.2007.09.006

Alberts B, Johnson A, Lewis J, et al (2002)Molecular biology of the cell. 4th edition. New York: Garland Science; Available from: https://www.ncbi.nlm.nih.gov/books/NBK21054/

Andersson CE, Mowbray SL (2002) Activation of ribokinase by monovalent cations. J Mol Biol 315:409–419. https://doi.org/10.1006/jmbi.2001.5248

Asatiani NV, Abuladze MK, Kartvelishvili TM, Bakradze NG, Sapojnikova NA, Tsibakhashvili NY, Tabatadze LV, Lejava LV, Asanishvili LL, Holman HY (2004) Effect of chromium(VI) action on Arthrobacter oxydans. Curr Microbiol 49:321–326

Asatiani N, Kartvelishvili T, Sapojnikova N et al (2018) Effect of the Simultaneous Action of Zinc and Chromium on Arthrobacter spp. Water Air Soil Pollut 229. https://doi.org/10.1007/s11270-018-4046-0

Atapaththu KSS, Rashid MH, Asaeda T (2016) Growth and oxidative stress of brittlewort (Nitella pseudoflabellata) in response to cesium exposure. Bull Environ Contam Toxicol 96:347–353. https://doi.org/10.1007/s00128-016-1736-4

Avery SV (1995a) Caesium accumulation by microorganisms: uptake mechanisms, cation competition, compartmentalization and toxicity. J Ind Microbiol 14:76–84. https://doi.org/10.1007/BF01569888

Avery SV (1995b) Microbial interactions with caesium—implications for biotechnology. J Chem Technol Biotechnol 62:3–16. https://doi.org/10.1002/jctb.280620102

Booth IR, Edwards MD, Miller S (2003) Bacterial ion channels. Biochemistry 42:10045–10053. https://doi.org/10.1021/bi034953w

Bossemeyer D, Schlosser A, Bakker EP (1989) Specific cesium transport via the Escherichia coli Kup (TrkD) K+ uptake system. J Bacteriol 171:2219–2221. https://doi.org/10.1128/jb.171.4.2219-2221.1989

Brown GR, Cummings SP (2001) Potassium uptake and retention by Oceanomonas baumannii at low water activity in the presence of phenol. FEMS Microbiol Lett 205:37–41. https://doi.org/10.1016/S0378-1097(01)00436-0

Bruins MR, Kapil S, Oehme FW (2000) Microbial resistance to metals in the environment. Ecotoxicol Environ Saf 45:198–207. https://doi.org/10.1006/eesa.1999.1860

Burger A, Lichtscheidl I (2018) Stable and radioactive cesium: a review about distribution in the environment, uptake and translocation in plants, plant reactions and plants' potential for bioremediation. Sci Total Environ 618:1459–1485

Chandrangsu P, Rensing C, Helmann JD (2017) Metal homeostasis and resistance in bacteria. Nat Rev Microbiol 15:338–350

Choudhury R, Srivastava S (2001) Mechanism of zinc resistance in Pseudomonas putida strain S4. World J Microbiol Biotechnol 17:149–153. https://doi.org/10.1023/A:1016666000384

Cook LL, Inouye RS, McGonigle TP, White GJ (2007) The distribution of stable cesium in soils and plants of the eastern Snake River Plain in southern Idaho. J Arid Environ 69:40–64

Cuello LG, Jogini V, Cortes DM, Perozo E (2010) Structural mechanism of C-type inactivation in K+ channels. Nature 466:203–208

Davies JS, Currie MJ, Wright JD, Newton-Vesty MC, North RA, Mace PD, Allison JR, Dobson RCJ (2021) Selective nutrient transport in bacteria: multicomponent transporter systems reign supreme. Front Mol Biosci 8:1–10

Djedidi S, Kojima K, Yamaya H, Ohkama-Ohtsu N, Bellingrath-Kimura SD, orothe., Watanabe I, Yokoyama T, (2014) Stable cesium uptake and accumulation capacities of five plant species as influenced by bacterial inoculation and cesium distribution in the soil. J Plant Res 127:585–597

Eisenberg D, and Crothers D (1979) Physical chemistry with applications to the life sciences (No. 541.3 E3)

Epstein W (2003) The roles and regulation of potassium in bacteria. Prog Nucleic Acid Res Mol Biol 75:293–320. https://doi.org/10.1016/S0079-6603(03)75008-9

Feile H, Porter JS, Slayman CL, Kaback HR (1980) Quantitative measurements of membrane potential in Escherichia coli. Biochemistry 19:3585–3590

Ferguson GP, Nikolaev Y, McLaggan D et al (1997) Survival during exposure to the electrophilic reagent N-ethylmaleimide in Escherichia coli: Role of KefB and KefC potassium channels. J Bacteriol 179:1007–1012. https://doi.org/10.1128/jb.179.4.1007-1012.1997

Follmann M, Becker M, Ochrombel I, Ott V, Krämer R, Marin K (2009) Potassium transport in corynebacterium glutamicum is facilitated by the putative channel protein CglK, which is essential for pH homeostasis and growth at acidic pH. J Bacteriol 191:2944–2952

Gadd GM, Griffiths AJ (1978) Microorganisms and heavy metal toxicity. Microb Ecol 4(303):317

Glasser R (1999) The water structure, effects of hydration. Chapter from book of Biophysics, 4th edn. Springer, Heidelberg, p 57

Grundling A (2013) Potassium Uptake Systems in Staphylococcus aureus: New Stories aboutt Ancient Systems. MBio 4:4–6. https://doi.org/10.1128/mBio.00407-13

Holman HYN, Perry DL, Martin MC et al (1999) Real-time characterization of biogeochemical reduction of Cr(VI) on basalt surfaces by SR-FTIR imaging. Geomicrobiol J 16:307–324. https://doi.org/10.1080/014904599270569

Ivshina IB, Peshkur TA, Korobov VP (2002) Efficient uptake of cesium ions by Rhodococcus cells. Microbiology 71:357–361. https://doi.org/10.1023/A:1015875216095

Jasper P (1978) Potassium transport system of Rhodopseudomonas capsulata. J Bacteriol 133:1314–1322. https://doi.org/10.1128/jb.133.3.1314-1322.1978

Juan CA, de la Lastra JMP, Plou FJ, Pérez-Lebeña E (2021) The chemistry of reactive oxygen species (Ros) revisited: outlining their role in biological macromolecules (dna, lipids and proteins) and induced pathologies. Int J Mol Sci. https://doi.org/10.3390/ijms22094642

Jung K, Krabusch M, Altendorf K (2001) Cs+ induces the kdp operon of Escherichia coli by lowering the intracellular K+ concentration. J Bacteriol 183:3800–3803. https://doi.org/10.1128/JB.183.12.3800-3803.2001

Kalabegishvili T, Murusidze I, Kirkesali E et al (2013) Gold and silver nanoparticles in Spirulina platensis biomass for medical application. Ecol Chem Eng S 20:621–631. https://doi.org/10.2478/eces-2013-0043

Kang SM, Jang SC, Heo NS et al (2017) Cesium-induced inhibition of bacterial growth of Pseudomonas aeruginosa PAO1 and their possible potential applications for bioremediation of wastewater. J Hazard Mater 338:323–333. https://doi.org/10.1016/j.jhazmat.2017.05.050

Kim I, Yang HM, Park CW, Yoon IH, Seo BK, Kim EK, Ryu BG (2019) Removal of radioactive cesium from an aqueous solution via bioaccumulation by microalgae and magnetic separation. Sci Rep 9:3–10

Koarashi J, Atarashi-Andoh M, Matsunaga T, Sanada Y (2016) Forest type effects on the retention of radiocesium in organic layers of forest ecosystems affected by the Fukushima nuclear accident. Sci Rep 6:1–11. https://doi.org/10.1038/srep38591

Latifi A, Ruiz M, Zhang CC (2009) Oxidative stress in cyanobacteria. FEMS Microbiol Rev 33:258–278. https://doi.org/10.1111/j.1574-6976.2008.00134.x

Linnik V, Korobova E, Brown J (2013) A historical outline of radionuclide contamination of the Yenisey floodplain based on landscape and radiometric survey. Geogr Environ Sustain 6:49–62. https://doi.org/10.24057/2071-9388-2013-6-2-49-62

Mahjoub S, Roudsari JM (2012) Role of oxidative stress in pathogenesis of metabolic syndrome. Casp J Intern Med 3:386–396

Mähler J, Persson I (2012) A study of the hydration of the alkali metal ions in aqueous solution. Inorg Chem 51:425–438. https://doi.org/10.1021/ic2018693

Marszalek P, Liu DS, Tsong TY (1990) Schwan equation and transmembrane potential induced by alternating electric field. Biophys J 58:1053–1058

Milo R, Phillips, R (2015) *Cell biology by the numbers*. Garland Science

Mironov KS, Sinetova MA, Shumskaya M, Los DA (2019) Universal molecular triggers of stress responses in cyanobacterium Synechocystis. Life 9:1–18. https://doi.org/10.3390/life9030067

Mosulishvili LM, Kirkesali EI, Belokobilsky AI, Khizanishvili AI, Frontasyeva MV, Gundorina SF, Opera CD (2002) Epithermal neutron activation analysis of blue-green algae Spirulina platensis as a matrix for selenium-containing pharmaceuticals. J Radioanal Nucl Chem 252:15–20

Nozadze M, Zhgenti E, Meparishvili M et al (2015) Comparative proteomic studies of Yersinia pestis strains isolated from natural foci in the Republic of Georgia. Front Public Heal 3:1–12. https://doi.org/10.3389/fpubh.2015.00239

Oh SY, Heo NS, Shukla S et al (2018) Multi-stress radioactive-tolerant Exiguobacterium acetylicum CR1 and its applicability to environmental cesium uptake bioremediation. J Clean Prod 205:281–290. https://doi.org/10.1016/j.jclepro.2018.09.077

Prindle A, Liu J, Asally M et al (2015) Ion channels enable electrical communication in bacterial communities. Nature 527:59–63. https://doi.org/10.1038/nature15709

Ram A, Lo AW (2018) Is smaller better? A proposal to use bacteria for neuroscientific modeling. Front Comput Neurosci 12:1–7. https://doi.org/10.3389/fncom.2018.00007

Ramos S, Kaback HR (1977) The electrochemical proton gradient in Escherichia coli membrane vesicles and its relationship to active transport. Biochem Soc Trans 5:23–25

Rhoads DB, Waters FB, Epstein W (1976) Cation transport in escherichia coli VIII. potassium transport mutants. J Gen Physiol 67:325–341. https://doi.org/10.1085/jgp.67.3.325

Sasaki H, Shirato S, Tahara T et al (2013) Accumulation of radioactive cesium released from Fukushima Daiichi nuclear power plant in terrestrial Cyanobacteria Nostoc commune. Microbes Environ 28:466–469. https://doi.org/10.1264/jsme2.ME13035

Schuldiner S, Kaback HR (1975) Mechanisms potentail and active transport in membrane vesicles from vesicles from Escherichia coli. Biochemistry 14:5451–5461. https://doi.org/10.1021/bi00696a011

Shaw G, Avila R, Fesenko S et al (2003) Chapter 11 Modelling the behaviour of radiocaesium in forest ecosystems. Radioact Environ 4:315–351. https://doi.org/10.1016/S1569-4860(03)80067-0

Sheahan JJ, Ribeiro-net L, Sussman MR (1992) Cesium-insensitive mutants of Arabidopsis thaliana. Plant J 3:647–656

Smirnov PR, Trostin VN (2007) Structures of the nearest surroundings of the K+, Rb +, and Cs+ ions in aqueous solutions of their salts. Russ J Gen Chem 77:2101–2107. https://doi.org/10.1134/S1070363207120043

Stautz J, Hellmich Y, Fuss MF, Silberberg JM, Devlin JR, Stockbridge RB, Hänelt I (2021) Molecular mechanisms for bacterial potassium homeostasis. J Mol Biol. https://doi.org/10.1016/j.jmb.2021.166968

Stingl K, Brandt S, Uhlemann EM, Schmid R, Altendorf K, Zeilinger C, Ecobichon C, Labigne A, Bakker EP, De Reuse H (2007) Channel-mediated potassium uptake in Helicobacter pylori is essential for gastric colonization. EMBO J 26:232–241

Stratford JP, Edwards CLA, Ghanshyam MJ, Malyshev D, Delise MA, Hayashi Y, Asally M (2019) Electrically induced bacterial membrane-potential dynamics correspond to cellular proliferation capacity. Proc Natl Acad Sci U S A 116:9552–9557

Suzuki Y, Kelly SD, Kemner KM, Banfield JF (2002) Nanometre-size products of uranium bioreduction. Nature 419:134–134. https://doi.org/10.1038/419134a

Takei T, Yamasaki M, Yoshida M (2014) Cesium accumulation of Rhodococcus erythropolis CS98 strain immobilized in hydrogel matrices. J Biosci Bioeng 117:497–500. https://doi.org/10.1016/j.jbiosc.2013.09.013

Tsibakhashvili NY, Kalabegishvili TL, Rcheulishvili AN, Murusidze IG, Rcheulishvili OA, Kerkenjia SM, Holman HYN (2009) Decomposition of Cr(V)-diols to Cr(III) complexes by arthrobacter oxydans. Microb Ecol. https://doi.org/10.1007/s00248-008-9476-6

Tsibakhashvili NY, Kalabegishvili TL, Rcheulishvili AN et al (2011) Effect of Zn(II) on the reduction and accumulation of Cr(VI) by Arthrobacter species. J Ind Microbiol Biotechnol 38(11):1803–1808. https://doi.org/10.1007/s10295-011-0967-y

Tsibakhashvili NY, Mosulishvili LM, Kalabegishvili TL, Pataraya DT, Gurielidze MA, Nadareishvili GS et al (2002b) Chromate-resistant and reducing microorganisms in Georgia basalts: their distribution and characterization. Fresenius Environ Bull 11(7):352–361

Ungar D, Barth A, Haase W, Kaunzinger A, Lewitzki E, Ruiz T, Reiländer H, Michel H (2001) Analysis of a putative voltage-gated prokaryotic potassium channel. Eur J Biochem 268:5386–5396

Valko M, Jomova K, Rhodes CJ et al (2016) Redox- and non-redox-metal-induced formation of free radicals and their role in human disease

Wackett LP, Dodge AG, Lynda BM, Ellis LBM (2004) Microbial genomics and the periodic table MINIREVIEW microbial genomics and the periodic table. Appl Environ Microbiol 70:647–655. https://doi.org/10.1128/AEM.70.2.647

Wang J, Zhuang S (2019) Removal of cesium ions from aqueous solutions using various separation technologies. Rev Environ Sci Biotechnol. https://doi.org/10.1007/s11157-019-09499-9

White PJ, Broadley MR (2000) Mechanisms of caesium uptake by plants. New Phytol 147:241–256

Yamamoto A, Yoshida S, Okumura H et al (2015) Local mat-forming cyanobacteria effectively facilitate decontamination of radioactive cesium in rice fields. J Smart Process 4:287–293. https://doi.org/10.7791/jspmee.4.287

Yang S, Han C, Wang X, Nagatsu M (2014) Characteristics of cesium ion sorption from aqueous solution on bentonite- and carbon nanotube-based composites. J Hazard Mater 274:46–52. https://doi.org/10.1016/j.jhazmat.2014.04.001

Yasunari TJ, Stohl A, Hayano RS et al (2011) Cesium-137 deposition and contamination of Japanese soils due to the Fukushima nuclear accident. Proc Natl Acad Sci U S A 108:19530–19534. https://doi.org/10.1073/pnas.1112058108

Yoshida S, Muramatsu Y, Steiner M (2000) Relationship between radiocesium and stable cesium in plants and mushrooms collected from forest ecosystems with different contamination levels. Proc 10th Symp Int Radiat Prot Assoc P11–244

Yu W, He J, Lin W et al (2015) Distribution and risk assessment of radionuclides released by Fukushima nuclear accident at the northwest Pacific. J Environ Radioact 142:54–61. https://doi.org/10.1016/j.jenvrad.2015.01.005

Zhang P, Idota Y, Yano K et al (2014) Characterization of cesium uptake mediated by a potassium transport system of bacteria in a soil conditioner. Biol Pharm Bull 37:604–607. https://doi.org/10.1248/bpb.b13-00871

Zok D, Blenke T, Reinhard S, Sprott S, Kegler F, Syrbe L, Querfeld R, Takagai Y, Drozdov V, Chyzhevskyi I, Kirieiev S, Schmidt B, Adlassnig W, Wallner G, Dubchak S, Steinhauser G (2021) Determination of characteristic vs anomalous 135Cs/137Cs isotopic ratios in radioactively contaminated environmental samples. Environ Sci Technol 55:4984–4991

Zheng J. and Trudeau MC (Eds) (2015). Handbook of Ion Channels (1st ed.). CRC Press. https://doi.org/10.1201/b18027